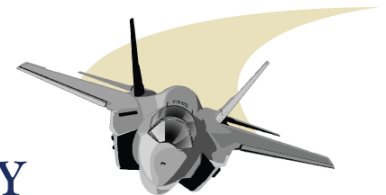


Characterization of nanoscale surface films in Molybdenum Disulfide

Harmandeep S. Khare and David L. Burris
Mechanical Engineering, University of Delaware



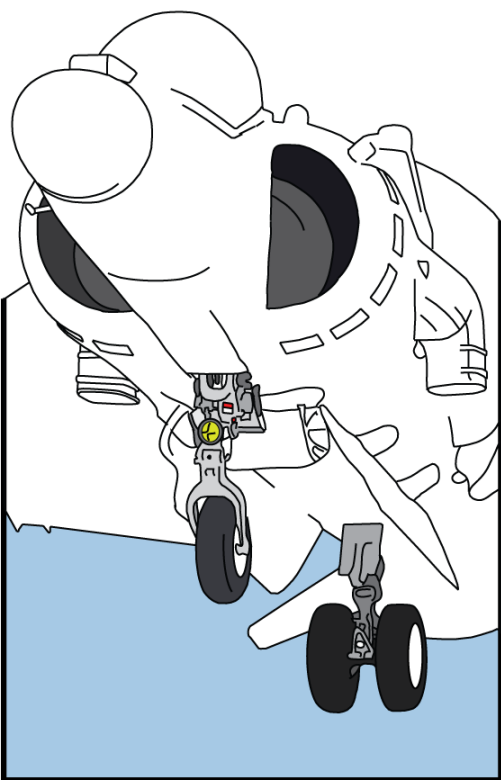
MATERIALS
TRIBOLOGY
LABORATORY



Tribology in extreme environments

Conventional lubricants such as oils and greases cannot be used in environments subject to extremes of temperature, humidity and particulate matter

Their limited applicability has motivated the use of solid lubricants, capable of sustained low friction, low wear sliding in extreme environments



Terrestrial tribology

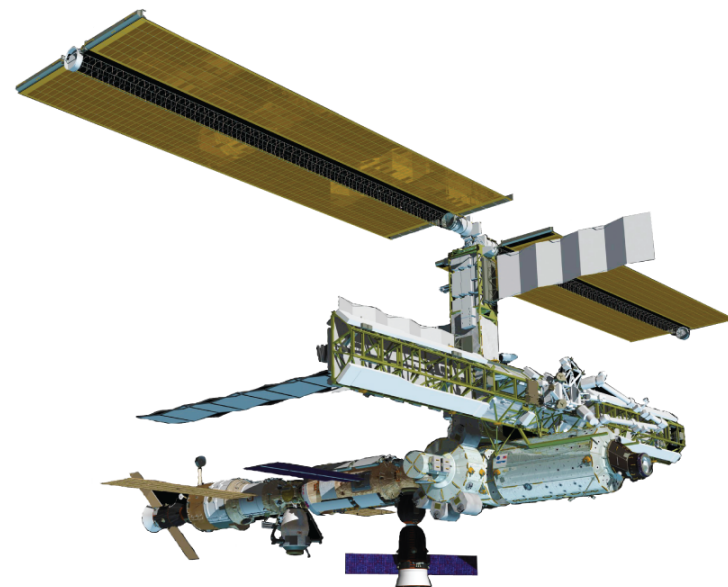
Extreme temperatures

Operability needs to be ensured irrespective of geographic location

Environmental conditions

Depending on location, moving parts subject to sandy or corrosive environment

Irrespective of operational conditions, frictional losses need to be minimized, if not terminated completely



Space tribology

Extreme temperatures

Deployment, positioning, power management, data collection and communication needed at near absolute zero temperatures

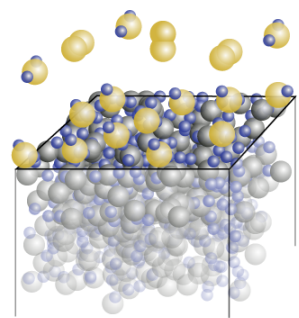
Environmental conditions

Ultra-high vacuum in space; atomic oxygen and radiation

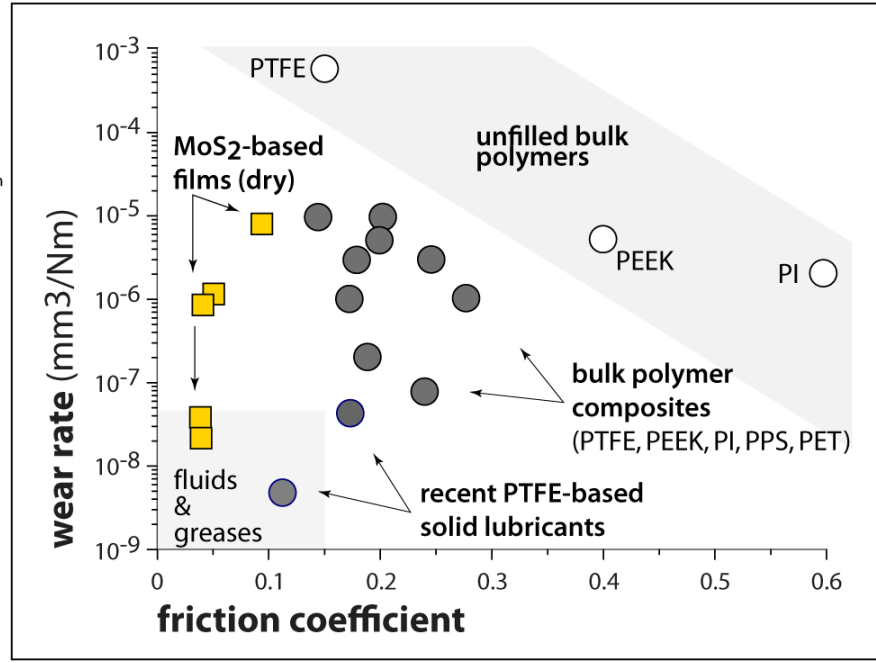
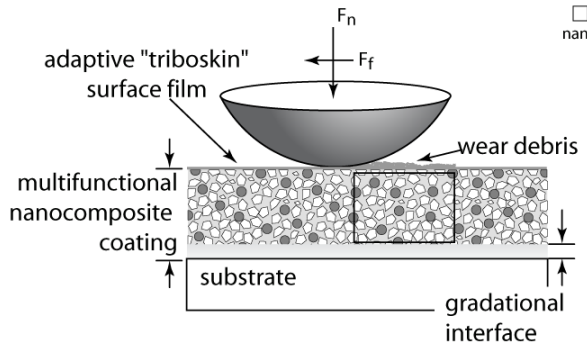
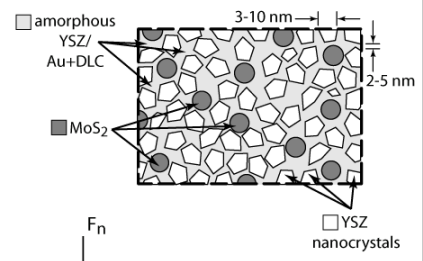
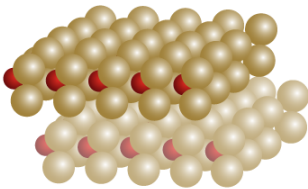
Added to harsh conditions, such equipment is nearly impossible to service

Solid lubricants and tribofilms

carbon films
(low friction in vacuum or air)
films of varying hybridization, crystallinity, hydrogen content, grain size

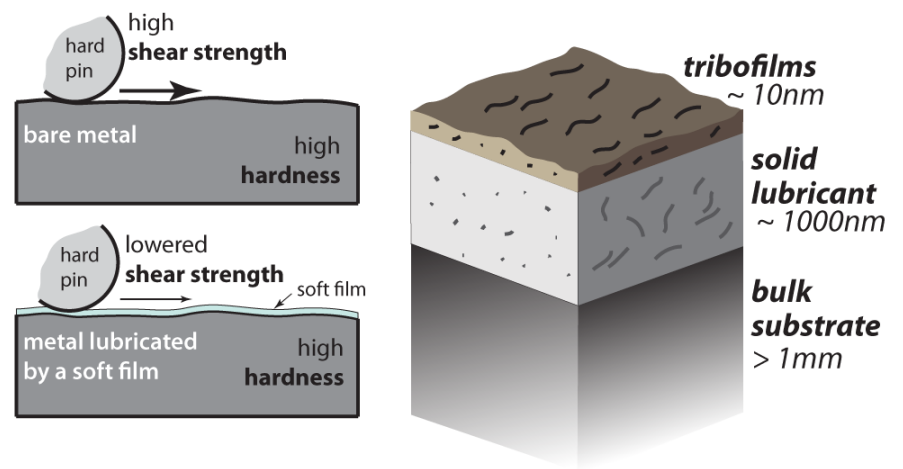


molybdenum disulfide
(low friction in vacuum)



From the classical adhesive theory of friction, a solid lubricant's ability to mimic the low friction behavior of liquid lubricants relies on presence of low-shear strength interfaces

Solid lubricants often undergo surface transformations during sliding, forming thin and ordered tribofilms

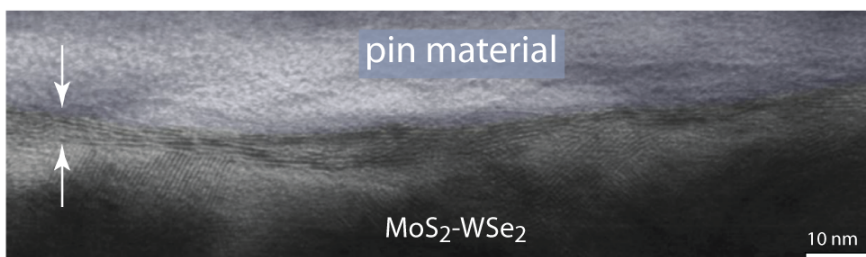
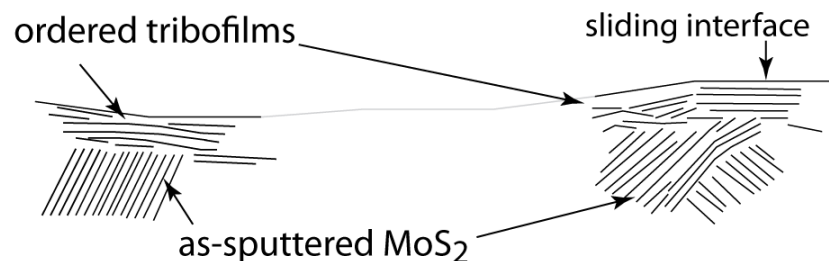
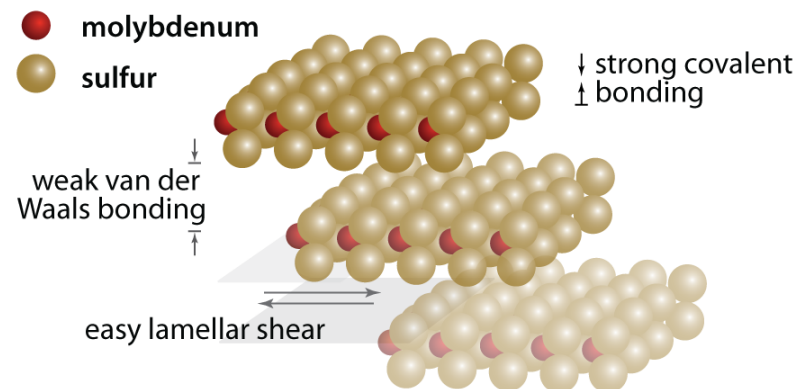


Molybdenum disulfide as a solid lubricant

Used extensively as a dry lubricant in a range of applications, especially for lubrication in space components, often in the form of thin sputtered coatings

Unique ability to provide ultra-low friction ($\mu < 0.01$) in **clean environment**; $\mu \sim 0.15$ in 'contaminated', humid air

Ultra-low friction widely accepted to originate from the easy shear of basal planes. Origin of low friction often likened to a sliding deck of cards



Hu et al. (2008)

Tribofilms in MoS₂

Recent TEM investigations have shown thin (of the order of 10nm) and ordered MoS₂ layers at the sliding interface. Structurally, these differ greatly from layers of MoS₂ buried under the real sliding interface

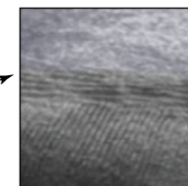
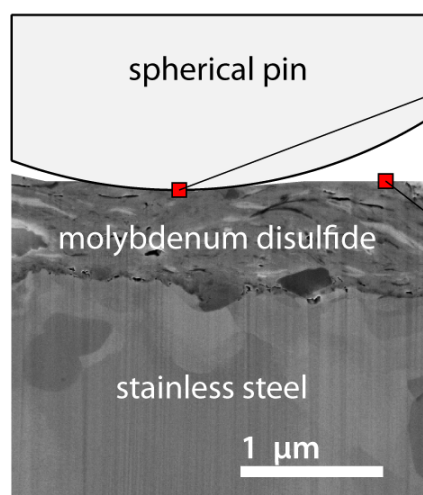
While yet largely uncharacterized, these thin tribofilms are believed to be crucial to frictional characteristics of MoS₂

A multi-scale approach to MoS₂ tribology

In order to characterize tribofilms and their contribution in reducing friction, a direct yet non-invasive probe of tribofilms at the relevant length-scales is required.

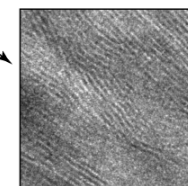
Surface nano-mechanical properties of unworn MoS₂ are compared with worn MoS₂ to highlight contributions from sliding-induced changes.

The perfectly ordered microstructure of single crystal MoS₂ is used as a control substrate, representing an idealized limit of the tribofilm microstructure.

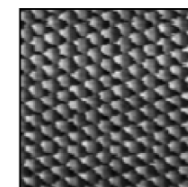


worn MoS₂
*anisotropic, ordered
lattice layers at surface*

Hu et al., 2008

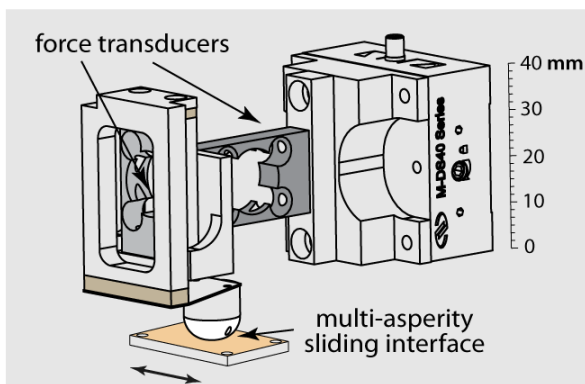


unworn MoS₂
*random (as-sputtered)
lattice orientation*



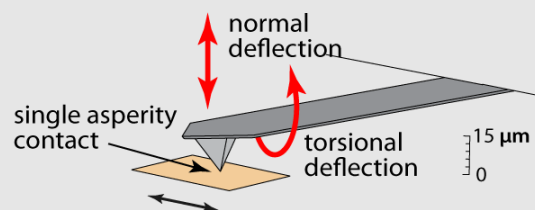
single crystal MoS₂
perfect lattice order

Zhang et al., 2010



interfacial sliding and multi-asperity plastic deformation at relatively high loads lead to formation of tribofilms

microtribometry



single-asperity contact measures highly localized surface-mechanical properties without appreciable damage from wear

nanotribology

Lateral force microscopy techniques are ideally suited in this role, capable of probing highly localized surface properties, without perturbing the surface itself.

A multi-scale approach to tribofilm characterization affords a chance to understand factors that influence tribofilm nanomechanics, and how these properties drive tribological response across the macro-scale.

Scanning probe mechanics of contact

$$W = \frac{V_{xf} - V_{xr}}{2}$$



$$W' = \frac{\partial W}{\partial V_y}$$

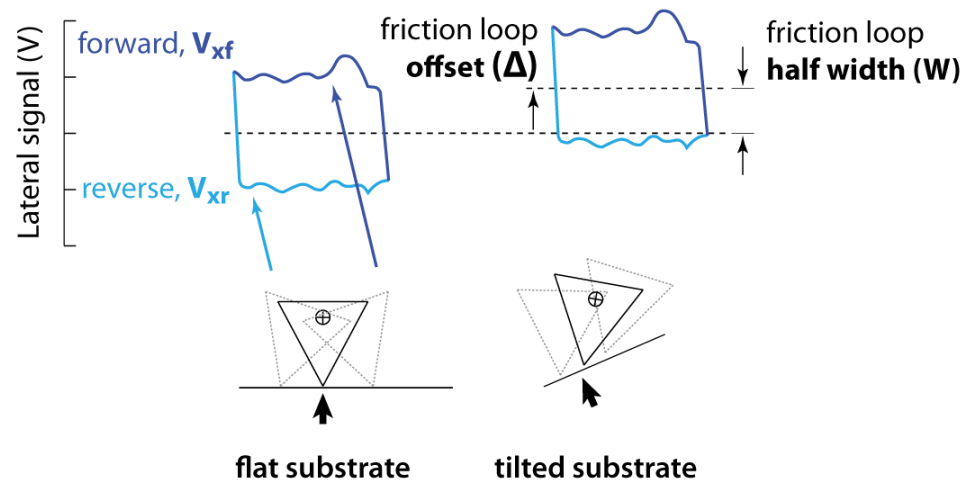
*change in loop-width
with load*

$$\Delta = \frac{V_{xf} + V_{xr}}{2}$$



$$\Delta' = \frac{\partial \Delta}{\partial V_y}$$

*change in loop-offset
with load*



Scanning probe mechanics of contact

$$W = \frac{V_{xf} - V_{xr}}{2}$$



$$W' = \frac{\partial W}{\partial V_y}$$

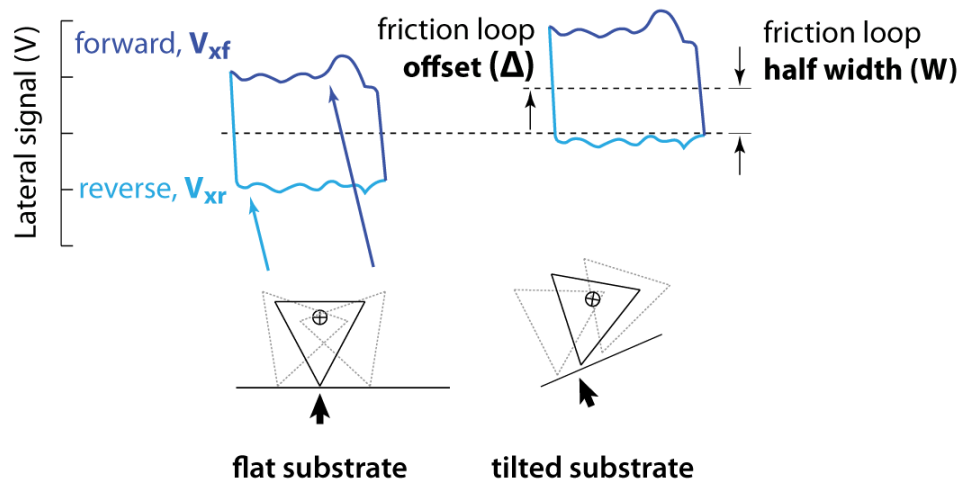
change in loop-width
with load

$$\Delta = \frac{V_{xf} + V_{xr}}{2}$$

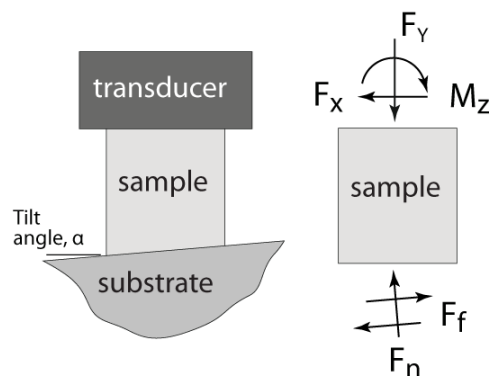


$$\Delta' = \frac{\partial \Delta}{\partial V_y}$$

change in loop-offset
with load



Transducer misalignments



$$F_{xf} = \mu F_n \cos(\alpha) - F_n \sin(\alpha)$$

$$F_{xr} = -\mu F_n \cos(\alpha) - F_n \sin(\alpha)$$

$$F_{yf} = F_n \cos(\alpha) + \mu F_n \sin(\alpha)$$

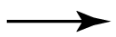
$$F_{yr} = F_n \cos(\alpha) - \mu F_n \sin(\alpha)$$

$$\tilde{\Delta} = 0.5 * \left(\frac{F_{xf}}{F_{yf}} + \frac{F_{xf}}{F_{yf}} \right)$$

$$\tilde{W} = 0.5 * \left(\frac{F_{xf}}{F_{yf}} - \frac{F_{xf}}{F_{yf}} \right)$$

Scanning probe mechanics of contact

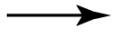
$$W = \frac{V_{xf} - V_{xr}}{2}$$



$$W' = \frac{\partial W}{\partial V_y}$$

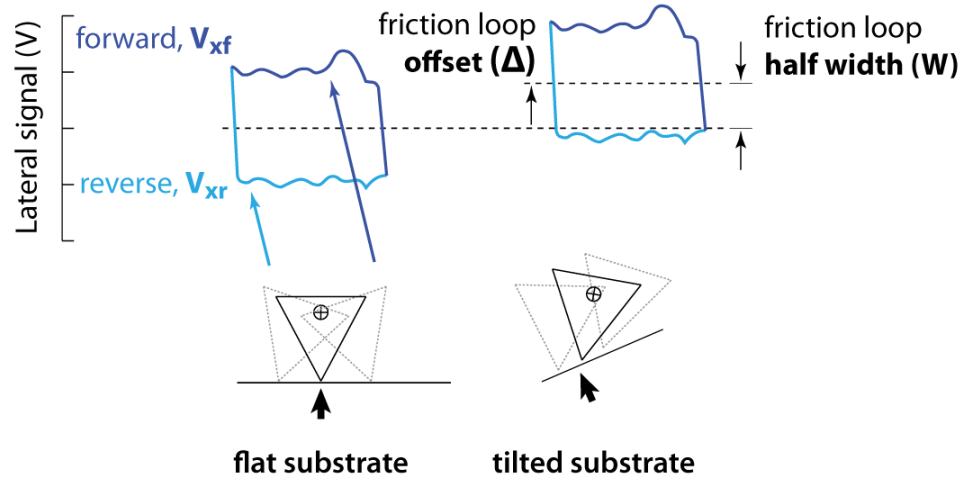
change in loop-width with load

$$\Delta = \frac{V_{xf} + V_{xr}}{2}$$

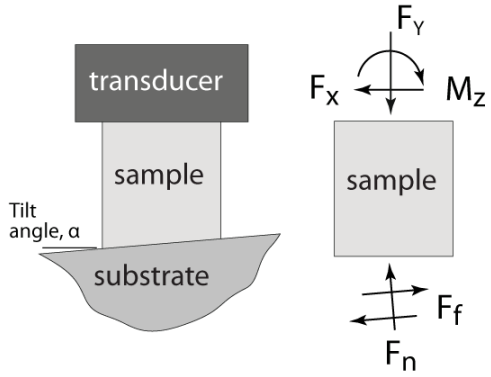


$$\Delta' = \frac{\partial \Delta}{\partial V_y}$$

change in loop-offset with load



Transducer misalignments



$$F_{xf} = \mu F_n \cos(\alpha) - F_n \sin(\alpha)$$

$$F_{xr} = -\mu F_n \cos(\alpha) - F_n \sin(\alpha)$$

$$F_{yf} = F_n \cos(\alpha) + \mu F_n \sin(\alpha)$$

$$F_{yr} = F_n \cos(\alpha) - \mu F_n \sin(\alpha)$$

$$\tilde{\Delta} = 0.5 * \left(\frac{F_{xf}}{F_{yf}} + \frac{F_{xf}}{F_{yf}} \right)$$

$$\tilde{W} = 0.5 * \left(\frac{F_{xf}}{F_{yf}} - \frac{F_{xf}}{F_{yf}} \right)$$

$$\frac{C_x}{C_y V_y} \cdot \frac{(V_{xf} + V_{xr})}{2} = \frac{C_x}{C_y} \cdot \frac{\Delta}{V_y}$$

$$\longrightarrow \frac{C_x}{C_y} \cdot \Delta' = \frac{\mu}{\cos^2 \alpha - \mu^2 \cdot \sin^2 \alpha}$$

$$\frac{C_x}{C_y V_y} \cdot \frac{(V_{xf} - V_{xr})}{2} = \frac{C_x}{C_y} \cdot \frac{W}{V_y}$$

$$\longrightarrow \frac{C_x}{C_y} \cdot W' = \frac{\sin \alpha \cdot \cos \alpha (1 + \mu^2)}{\cos^2 \alpha - \mu^2 \cdot \sin^2 \alpha}$$

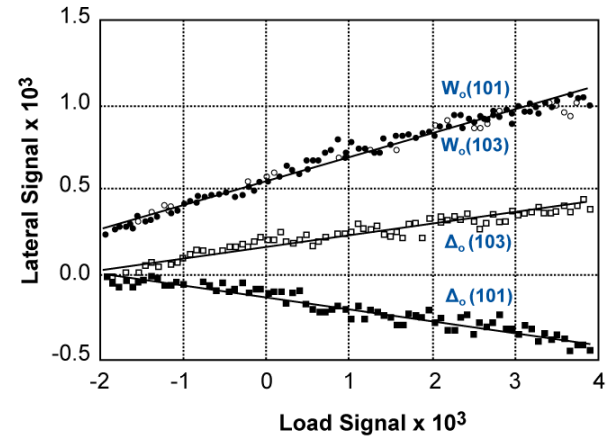
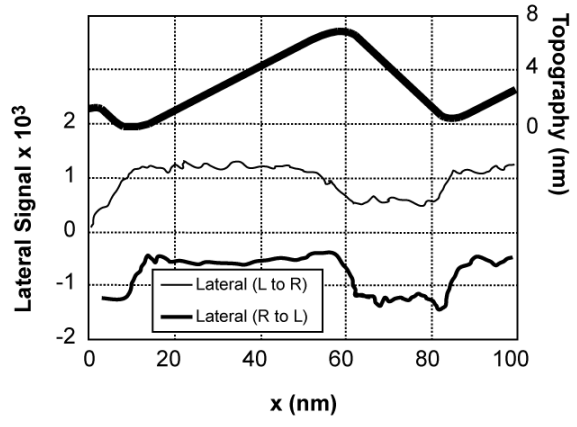
$$\frac{2 \Delta'}{W' \sin 2\alpha} = \mu + \frac{1}{\mu}$$

Two-slope method of lateral force calibration

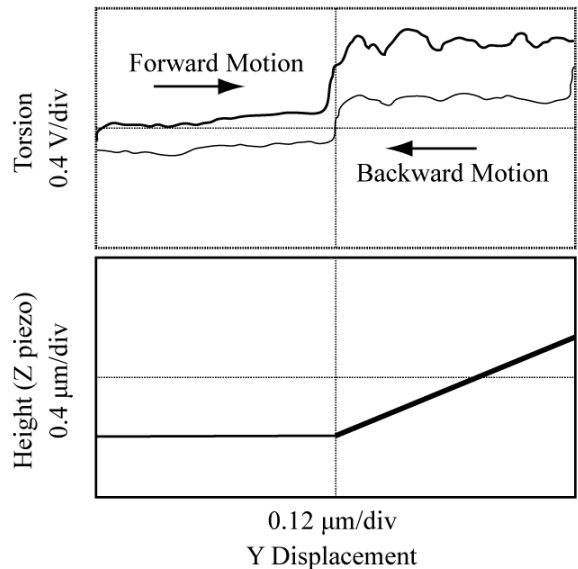
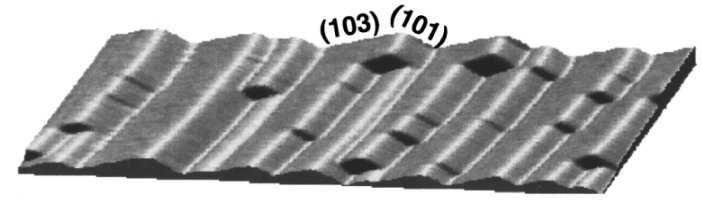
The "wedge" method (Ogletree et al. 1996, right) utilized substrates with known wedge angles to extract values of friction coefficient and force calibration constants. Friction coefficient is evaluated using the expression:

$$\mu + \frac{1}{\mu} = \frac{2 \Delta'}{W' \sin 2\alpha}$$

Effects of cross-talk between normal and lateral transducers eliminated through a two-slope calibration procedure.



The Ogletree method relies on a calibration substrate (SrTiO₃) with known ridge angles (14°, -12.5°).



Varenberg et al. (2003) (left) employ a silicon calibration grating, obtaining friction loop offset and width on a flat and inclined surfaces, using single-load sliding.

Aside from requiring calibration standards, these techniques require the calibration process as a separate, preceding step to quantitative friction measurement.

Complexity of SPM systems render lateral measurements prone to large uncertainty; a separation of the calibration and measurement allows these uncertainties to propagate in evaluated lateral calibrations and forces.

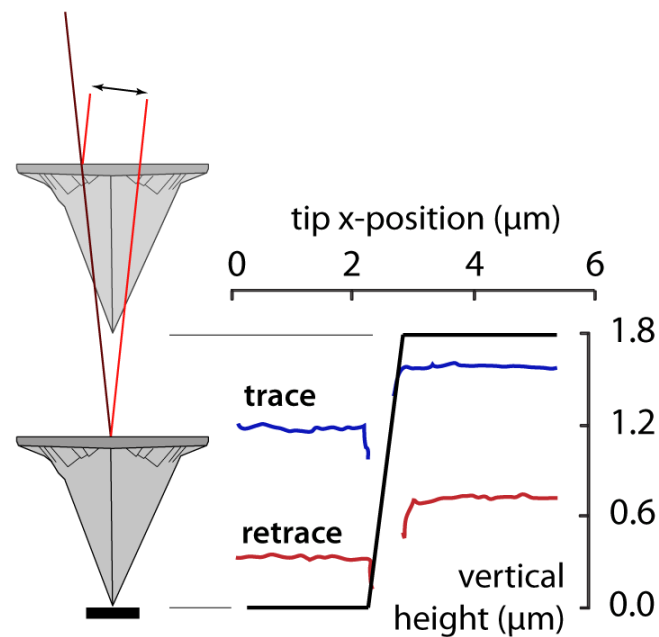
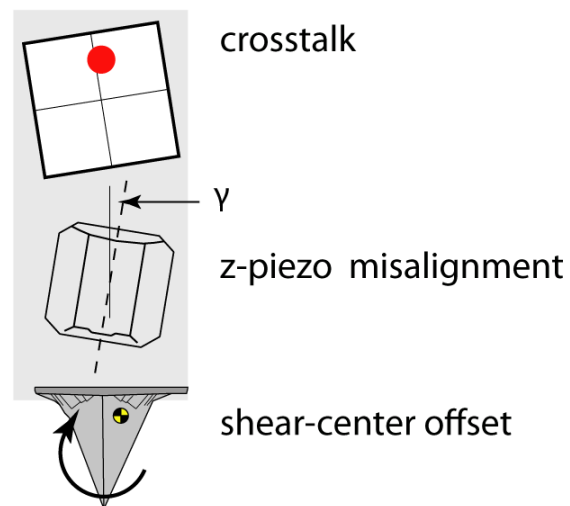
Sources of Error

In addition to photodiode induced crosstalk, factors such as piezo stack misalignment, tip shear offset, etc., add a degree of stochastic uncertainty in evaluated values of friction and calibration constants from a traditional calibration approach

A misalignment between the z-piezo travel axis and the plane of tip-travel introduces an error in load-dependent variation of friction-loop offset.

A lateral force measurement artifact identified by the LFM community notes false variations in lateral signal due to the vertical displacement of the z-piezo .

Small variations in z-piezo position change optical path of the laser, giving rise to differences in actual calibration values



Lateral force calibration

A method of calibration has been designed to help circumvent instrument misalignment and repeatability issues; torsional/lateral stiffness calibration is performed during measurement scanning on actual substrates.

Lateral force measurements are performed on the surface wedged at two complimentary angles.

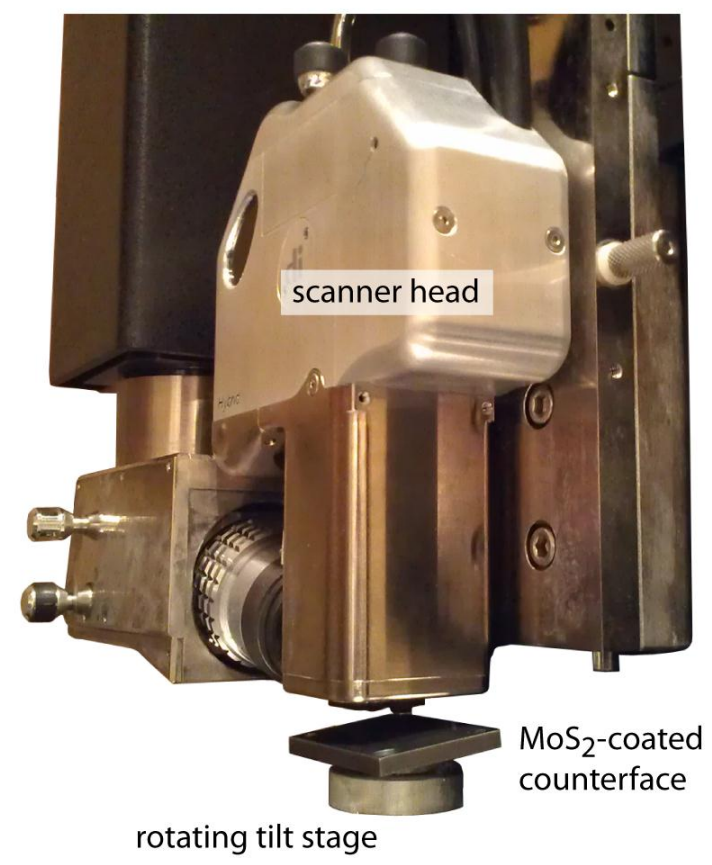
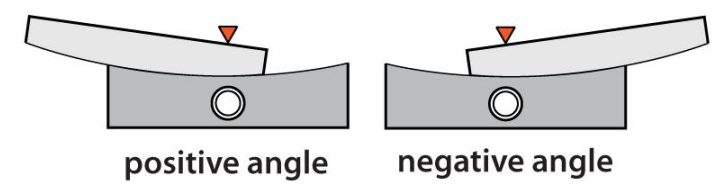
Equations of force-balance at the sliding contact are used to solve for four unknowns: friction coefficients, misalignment angle and the ratio of lateral to normal calibration constant.

$$\left[\frac{C_x}{C_y} \right] \cdot W' = \frac{\mu}{\cos^2(\alpha - \gamma) - \mu^2 \cdot \sin^2(\alpha - \gamma)}$$

$$\left[\frac{C_x}{C_y} \right] \cdot \Delta' = \frac{\sin \alpha \cdot \cos(\alpha - \gamma) (1 + \mu^2)}{\cos^2(\alpha - \gamma) - \mu^2 \cdot \sin^2(\alpha - \gamma)}$$

Unknowns:
 $\mu_1, \mu_2,$
 $C_x/C_y, \gamma$

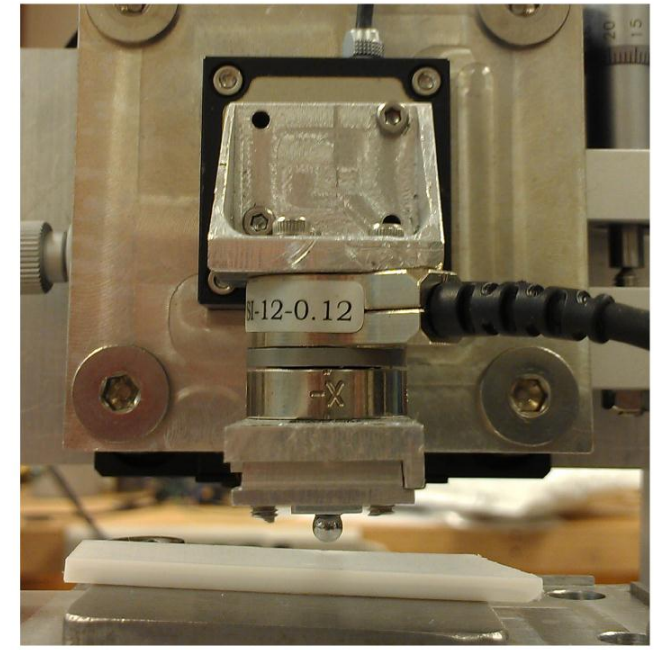
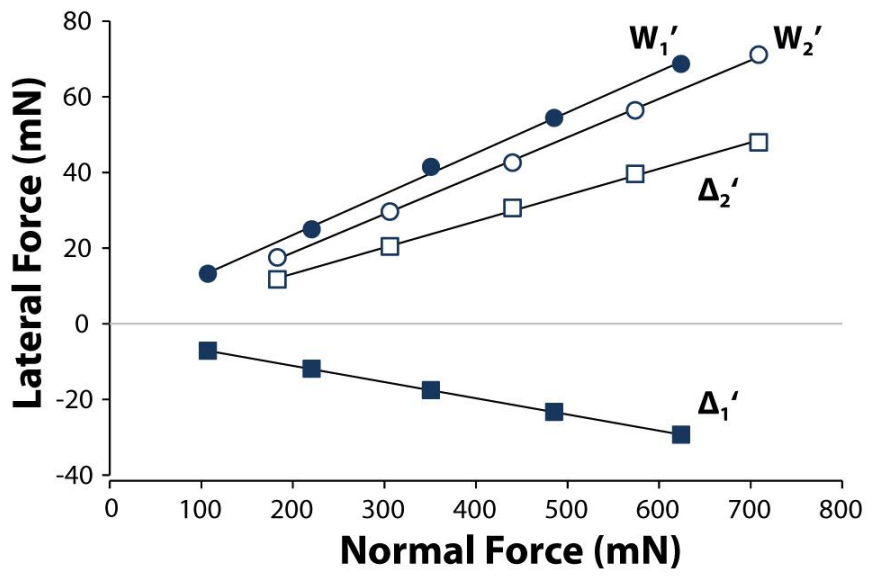
An iterative solution is obtained for the four unknowns, minimizing the standard deviation between the four values of C_x/C_y without a constraint on values of friction coefficient



Validation of method

In order to validate the proposed in-situ method of calibration, similar measurements were performed on a well-characterized microtribometer.

Normal and lateral force 'calibration constants' for the 6-channel load cell fitted to the tribometer were known a-priori, and values obtained by the in-situ calibration were compared with these.



Calibrated $C_x/C_y = 1$
 Evaluated $C_x/C_y = 0.98141$ ($\sigma \sim 10^{-6}$)

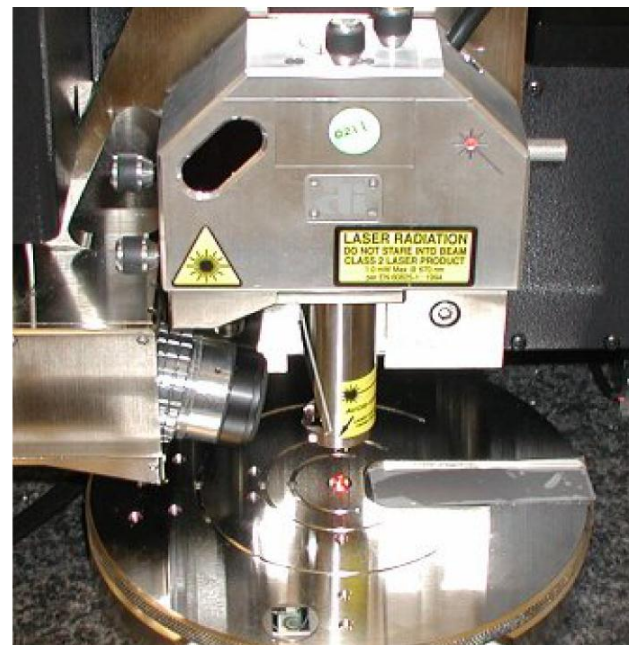
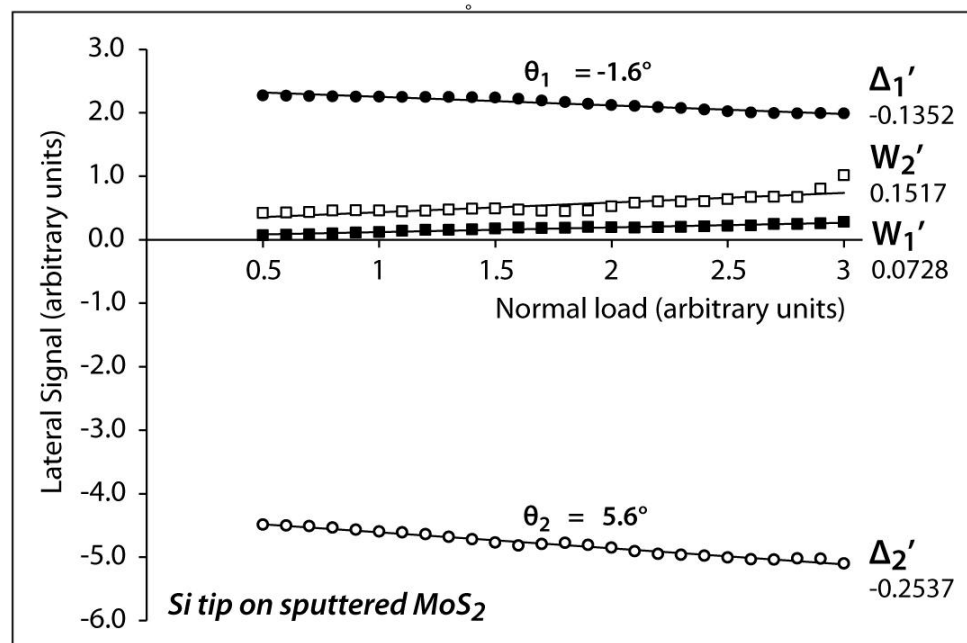
$\mu = 0.1$ $\gamma = -0.16^\circ$

Close proximity of the evaluated calibration to the actual values shows the applicability and accuracy of in-situ calibration.

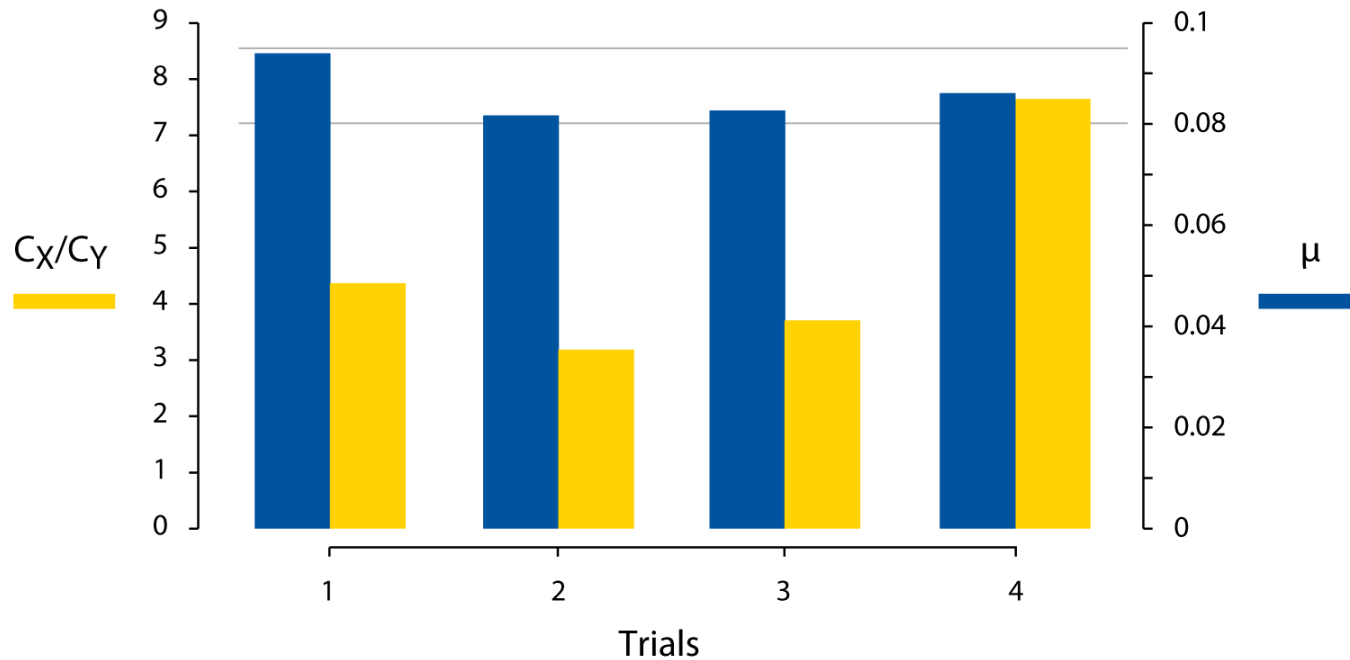
Measurement deviation on AFM

Convolution of uncertainties and misalignments, actual measurements on an AFM show large deviations from the predicted, ideal behavior

Loop-offset slopes obtained along two opposing angles may yield slopes with similar signs - this may be thought to arise from larger misalignment angles within the instrument piezo-stack



A lack of fidelity between successive measurements underscores the need for in-situ calibration which also accounts for secondary misalignments.



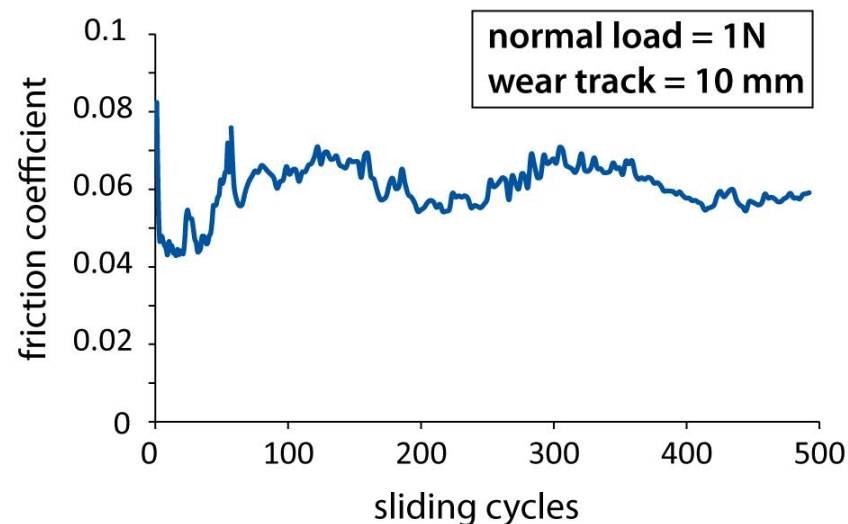
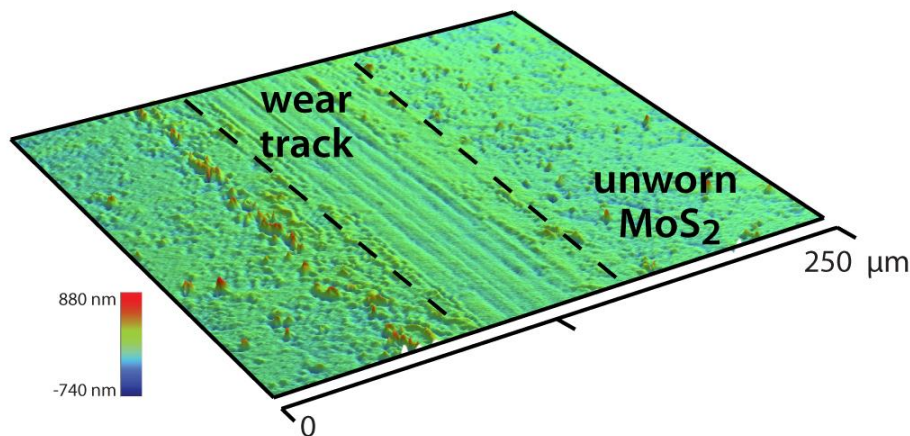
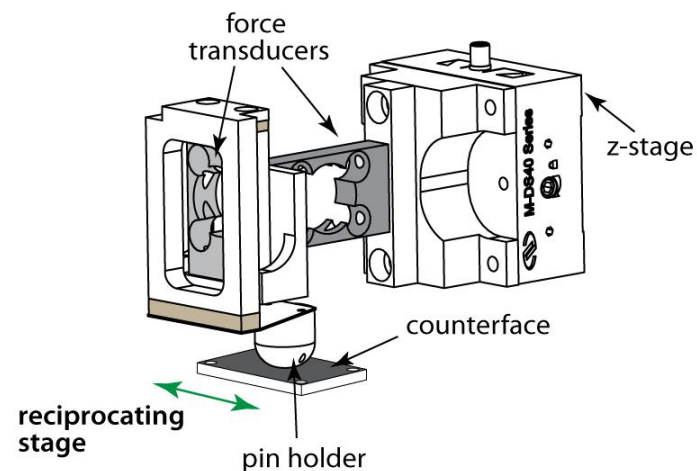
Variations in measurement-to-measurement values of calibration constant highlight the uncertainties associated with single-calibration friction measurement

In order to obtain greater measurement confidence in the quantitative values of friction, lateral calibration must be performed in-situ, while a friction measurement is being made

Macrotribological testing

Wear tracks for nanotribological characterization were created on a custom-tribometer. 1 μm thick MoS_2 coatings were commercially sputtered (Tribologix Inc.); a 10mm wear track was created in lab-air conditions after a sliding duration of 500 cycles.

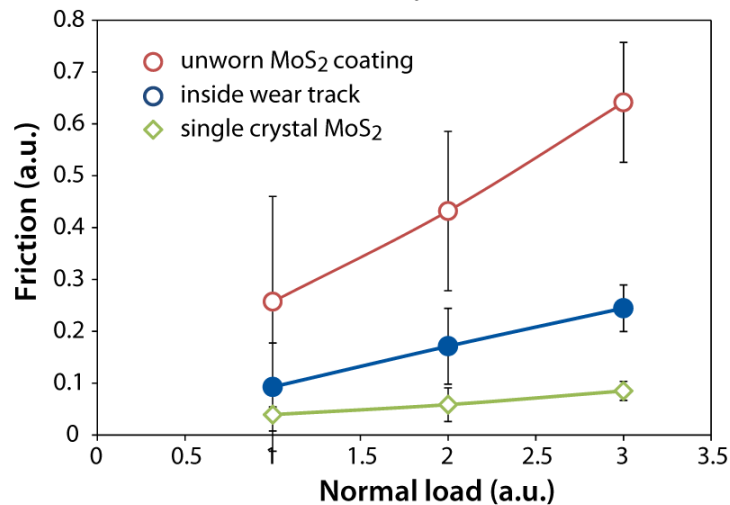
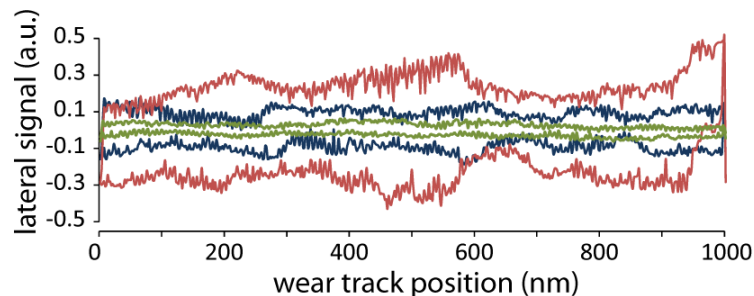
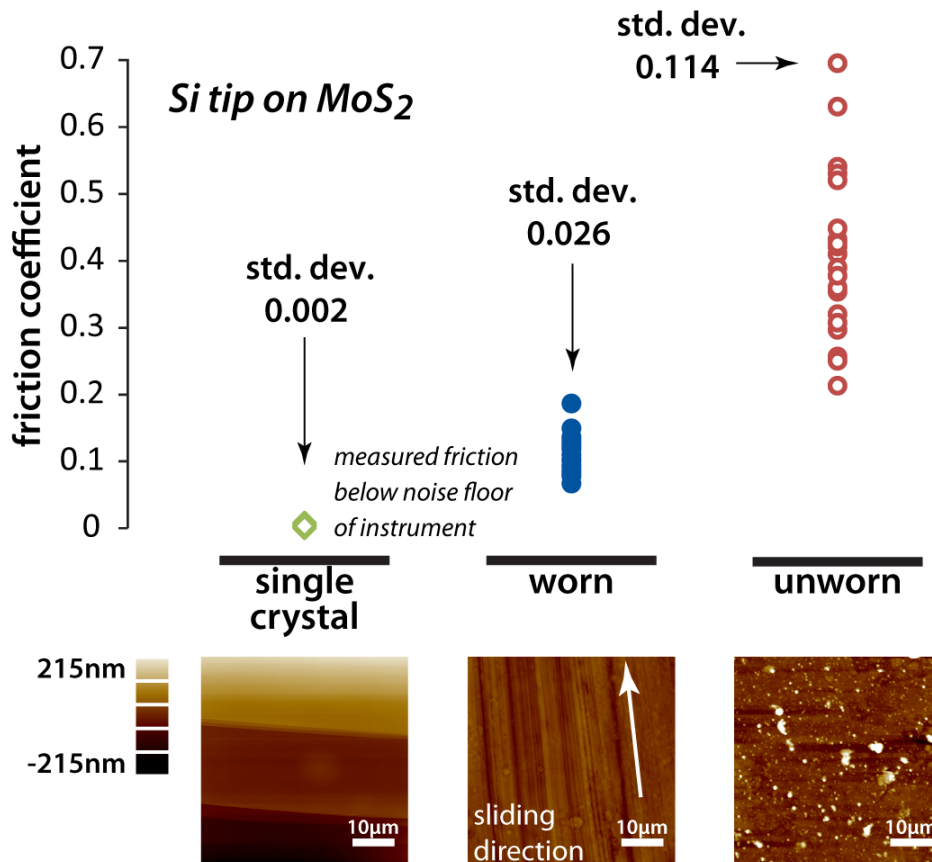
In order to facilitate low-wear sliding and propensity of low-shear tribofilms to form, macro-scale sliding was performed at a substrate temperature of 100°C, yielding a nominal friction coefficient of 0.06



Lateral Force Microscopy

All nanotribological measurements were made in lab-air conditions; friction measurements were derived from one-line scans across a 1 μm wear track.

Nano-friction measurements on the three microstructurally-different surfaces of MoS_2 were performed at 25 distinct locations on a local area; these provide a measure of both instrument repeatability and of the local property variations of heterogeneous surfaces.



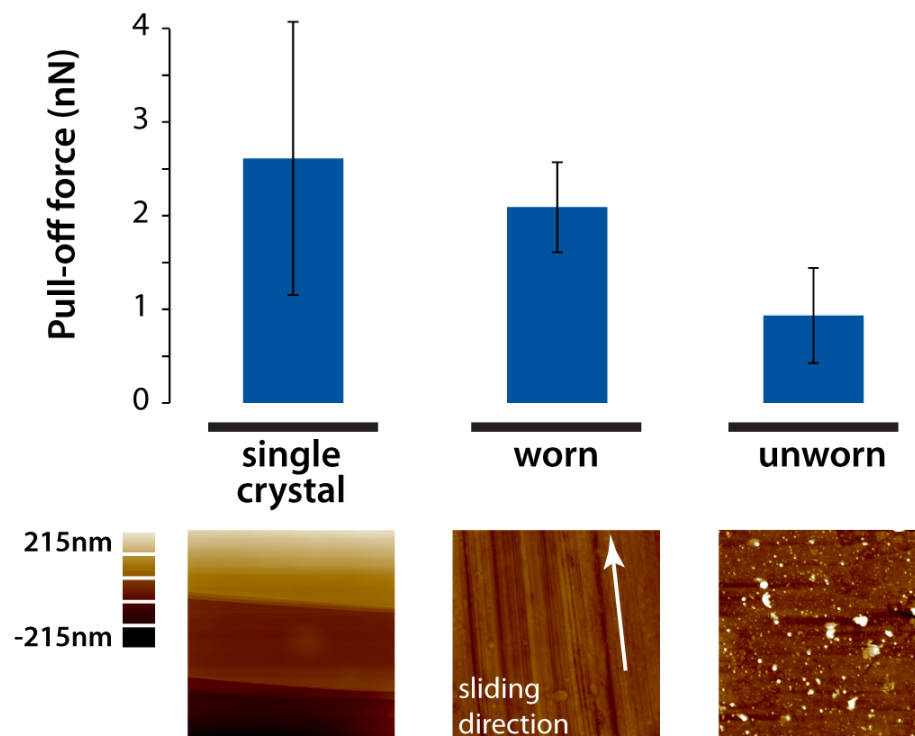
A trend of decreasing friction is seen between unworn, worn and single crystal MoS_2 .

Further, large spatial variation in value of friction coefficient is seen for unworn MoS_2 possibly indicating large heterogeneity in surface properties.

Pull-off force measurements were performed with Si_3N_4 tips in ambient conditions

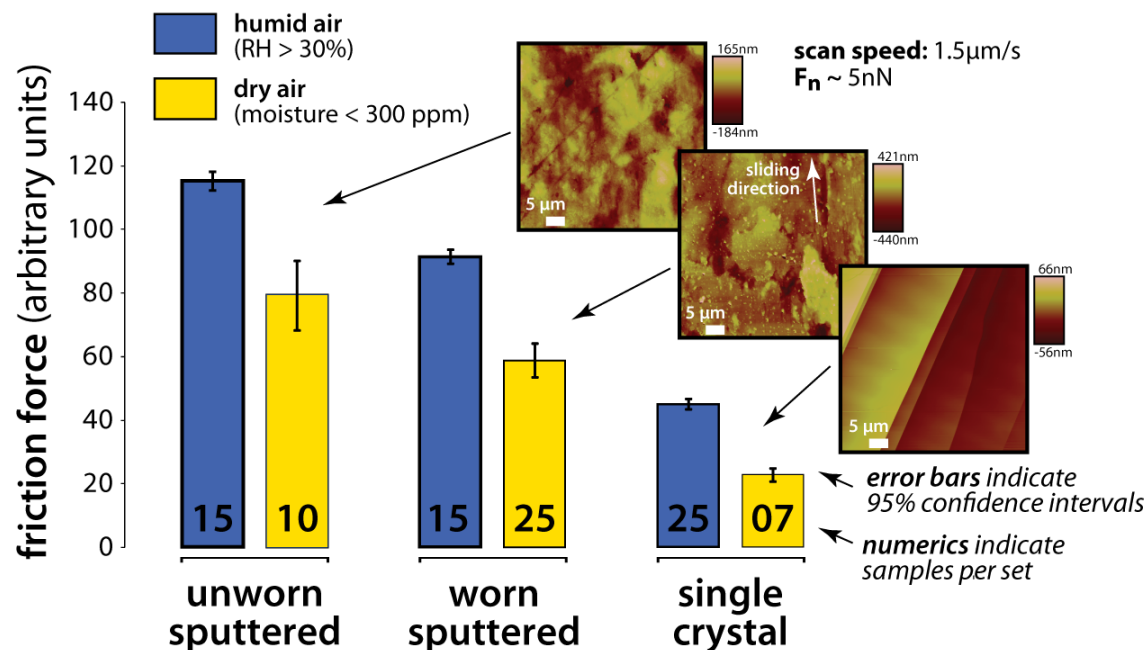
Experimental results suggest that **pull-off force increases with the orientation** of MoS_2 lamellae:

Adhesion values are observed to be lowest for unworn, sputtered coatings and highest for basal-plane single crystal.



Nanotribological studies on worn and unworn sputtered MoS₂ films show quantitative differences in nano-friction as a consequence of the formation of tribofilms.

Similar measurements performed at single-load values have also shown differences in the nano-friction in different environments; friction was consistently lower in dry air than humid air, which the trend of reducing friction was maintained between unworn, worn and single crystal MoS₂.



Measurements similar to those presented, made in varying environments can be expected to elucidate the role of environment on friction of tribofilms.

Further, varying the sliding environment during macro-scale sliding could be expected to yield tribofilms with varying microstructures and correspondingly different nanotribological and nanomechanical properties.

Lateral force microscopy techniques are ideally suited for characterizing the properties of oriented solid lubricant tribofilms, however, the lack of repeatability in existing calibration techniques makes this difficult.

An in-situ method of lateral force calibration is developed that enables cantilever calibration during friction measurements, providing a direct and robust measure of nano-scale friction.

When applied to MoS₂ tribofilms, friction is seen to decrease due to the sliding-induced formation of tribofilms. Future work will seek to build on these results to probe environmental dependence of both tribofilm properties and formation mechanisms.

Acknowledgement

The authors gratefully acknowledge the AFOSR (YIP FA9550-10-1-0295) and the University of Delaware Research Foundation (UDRF) for financial support

